International Research Journal of Engineering and Technology (IRJET) e-ISSN: 2395-0056
Volume: 10 Issue: 11 | Nov 2023 www.irjet.net p-ISSN: 2395-0072

Detection of Skin Diseases based on Skin lesion images

Kiran[1], Gurjit Kaur[2], Priyanka Arora[3]

[1]M.Tech (Computer Science & Engineering), GNDEC Ludhiana, Punjab, India
[2]Assistant Professor, Dept. of Computer Science &Engineering, GNDEC Ludhiana, Punjab, India
[2]Assistant Professor, Dept. of Computer Science &Engineering, GNDEC Ludhiana, Punjab, India

---

Abstract - *The largest organ of our human body is skin and skin cancer is the most predominant type of cancer that influences millions of people per annum. The survival rate of patients decreases steeply if cancer is not detected in early stages. However, early detection of cancer is a very strenuous and costly process. The skin cancer dataset consists of types of malignant skin cancer datasets. According to researchers in earlier stages, it is hard to detect due to minute differences compared to normal skin lesions. Therefore, the identification of cancerous skin lesions in the early stages is a difficult matter. In this process, we are going to discuss various technologies that can be used for skin cancer detection and classification and their results. The common approach for early detection of skin lesions is divided into four steps they are as follows: Data Collection, pre-processing, feature selection, and classification. The deep learning algorithm is used to identify skin cancer disease. It will help to easily identify earlier stages of skin cancer.*

Key Words: Data Collection, Pre-Processing, Feature Selection, Classification, Deep Learning

1. INTRODUCTION

The incidence of cancer is on the rise in the contemporary world, with each passing day[1]. A considerable portion of the population is confronted with the challenge of cancer. The treatments employed during this period are known for their demanding nature. Cancer manifests in various stages, and early detection provides a chance for a successful recovery. As the ailment advances, the challenges become more pronounced. The path of cancer treatment is notably strenuous, involving a series of chemotherapy sessions, potential surgical interventions, and subsequent radiation therapy. Cancer can arise in any bodily region, and differentiating between external and internal organ cancers reveals varying cure rates, with external organ cancers generally exhibiting a higher likelihood of successful treatment in comparison to internal organ cancers [2]. This research primarily centers on skin cancer, specifically concentrating on the detection of skin cancer through image analysis. The process encompasses several distinct phases of identification: Data collection, pre-processing, Model selection, model training, model evaluation, fine tuning and classification. A range of skin cancers can be identified, encompassing brain, colon, lung, breast, uterus, cervical, bladder, skin, liver, kidney, thyroid, and pancreatic cancer. Nevertheless, this work places specific emphasis on melanoma, a type of skin cancer. The procedure involves multiple sequential stages: pre-processing, where images are prepared for analysis; which isolates relevant areas, feature selection, identifying key characteristics; and classification; categorizing images based on these features. Skin cancer can manifest in various forms, including squamous cell carcinoma and basal cell carcinoma, Often requiring more comprehensive treatment strategies. Regardless of the specific cancer type, the disease stages play a pivotal role, spanning from stage 1 to stage 4. Higher success rates in recovery are typically observed in stages 1 to 3, while stage 4 presents lower chances of healing. Melanoma, a distinct type of skin cancer, poses notably high mortality risks and contributes significantly to overall fatalities. The primary objective is the precise identification and classification of skin cancer, with a particular emphasis on melanoma. Skin cancer, including melanoma, is frequently associated with excessive sun exposure. Non-melanoma skin cancers encompass basal cell carcinoma and squamous cell carcinoma. The proposed approach encompasses a comprehensive workflow covering all phases of cancer cell identification, from initial processing to classification. Incorporating textural features enhances the accuracy of classification algorithms. By comparing diverse classification algorithms, the most suitable one can be determined for various stages of melanoma detection. The suggested method showcases high accuracy using support vector machines. However, potential improvements can be achieved by introducing additional feature selection methods and broadening the scope of considered features beyond basic statistics like area, mean, standard deviation, and variance. Future methodologies might involve incorporating a more extensive array of features to enhance the classification rate. Although melanoma is less prevalent, its high fatality rate significantly contributes to skin cancer-related deaths. Early detection during the initial stages is pivotal for successful recovery, as delayed diagnosis escalates the risk of metastasis. Conventional detection methods involve manual examination by medical professionals, such as dermoscopy.

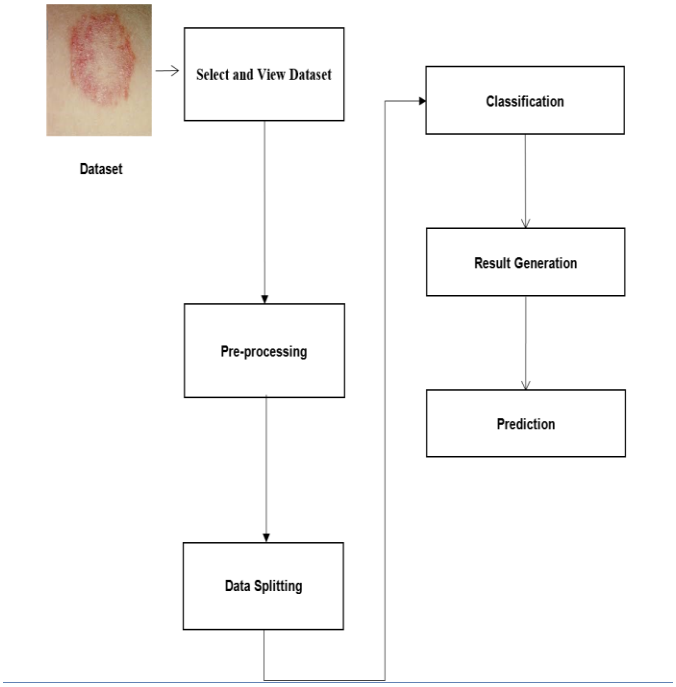

Figure 1: Proposed architecture for skin diseases classification.

1.1: Related Work

The frequency of cancer cases is increasing in the modern world, with each passing day[1]. The ongoing research highlights the various approaches utilized in terms of the identification and categorization of cutaneous malignancies[2]. These approaches encompass a spectrum of methods that are utilized throughout various stages, starting from initial pre-processing and data refinement, and advancing through the extraction of distinctive features[3] [4] [5]. The system was then evaluated by different evaluation metrics on ISIC 2016, ISIC 2017, ISIC 2018, ISIC 2019, and PH2 datasets[6] [7] [10]. The ultimate phase involves classification, in which machine learning techniques assume a crucial role by providing an advanced mechanism for managing extensive and intricate datasets.

2. Proposed Method

The newly introduced model aims to address the limitations present in the current system. This system enhances the precision of neural network results by employing a deep learning-based algorithm to classify different types of skin cancer within a digital image dataset. The overall classification performance is greatly enhanced, leading to a more dependable and precise identification of cancerous images.

2.1: Datasets

The dataset, comprised of images depicting both cancerous and non-cancerous cases, was sourced from the 'International Skin Imaging Collaboration (ISIC) images repository [26]. ISIC is a collaborative initiative between academic and industrial entities, aiming to facilitate the development of digital skin imaging applications that can contribute to the early detection of melanoma. ISIC focuses on establishing principles that address the terminology, technology, and techniques used in skin imaging, with particular emphasis on critical issues such as interoperability and privacy.The ISIC 2019 repository encompasses a dataset of 25,000 images, showcasing various types of cancerous and non-cancerous conditions. In the proposed ensemble approach for binary class classification, 3000 malignant and 2800 benign images were utilized. Given the limitation of benign images, an equal number of malignant images were selected to prevent algorithmic bias. The dataset was split into training data, which accounts for 80% of the total images, with the remaining images allocated for the test data. Considering that the dataset encompasses images of varied sizes, a resizing operation was conducted to standardize the images to 224 × 224 × 3 dimensions in the proposed approach.

2.2: Deep Neural Network

To create the proposed ensemble, two distinct deep neural network models based on convolution, namely, CNN and ResNet50 were developed. The following outlines the architectural development specifics for each model:

CNN: CNN stands for Convolutional Neural Network. It is a type of deep learning algorithm that has been particularly effective in areas such as image recognition and classification. CNNs are well suited for analyzing visual imagery due to their unique architecture, which allows them to automatically detect features in the input images and learn the relevant patterns. They consist of multiple layers, including convolutional layers, pooling layers, and fully connected layers, each serving different purposes in the process of feature extraction and classification. CNNs have played a crucial role in various tasks such as object recognition, image classification, and facial recognition.

RESNET-50: ResNet-50 is a specific variant of the Residual Network (ResNet) architecture. ResNet is a deep learning model that has demonstrated significant success in various computer vision tasks, particularly in image recognition and classification. ResNet-50 specifically refers to a ResNet model that consists of 50 layers, including convolutional layers, batch normalization, and rectified linear unit (ReLU) activations, along with shortcut connections that enable the flow of information across several layers more efficiently.ResNet-50 is known for its ability to address the vanishing gradient problem that often arises in very deep neural networks, allowing the successful training of extremely deep models. This architecture has been widely used in various applications, including image classification, object detection, and image segmentation tasks.

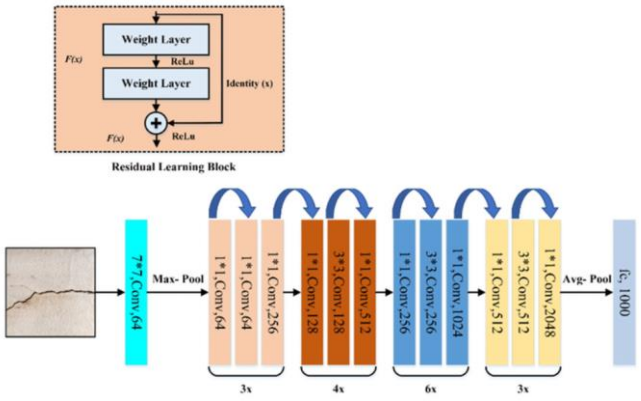

Figure 2: The architecture of Resnet-50.

Res-net models, residual block F(X) can be expressed mathematically as:

$$Y = F(X, \{Wi\}) + X \quad (1)$$

In the given equation Y is the output, X is the input, and F is the function that is applied to any input that is passed to the residual block. It has weight layers represented by Wi in which i must be greater than 1 but less than the number of layers present in the residual block. However, when several layers are equal to 2 then the term F(X, Wi) can be dumbed down and written as:

$$F(X,\{Wi\}) = W2\sigma(W1X) \quad (2)$$

where σ represents the ReLU activation function used by the model. Another non-linearity added with identity mapping after the addition is

F(X) = σ(Y) it doesn't use extra parameters. The building block of a residual network can be constructed as:

$$Y = F(Xi\{Wi\}) + WsX \quad (3)$$

where Y and X are the output and input vector, F is the residual mapping that has to be learned. If the dimensions of X and F are not equal, linear projection WsX can be performed by the given shortcut connections so that dimensions can be matched. Layers of Resnet are grouped in 4 parts as shown in Figure 3.

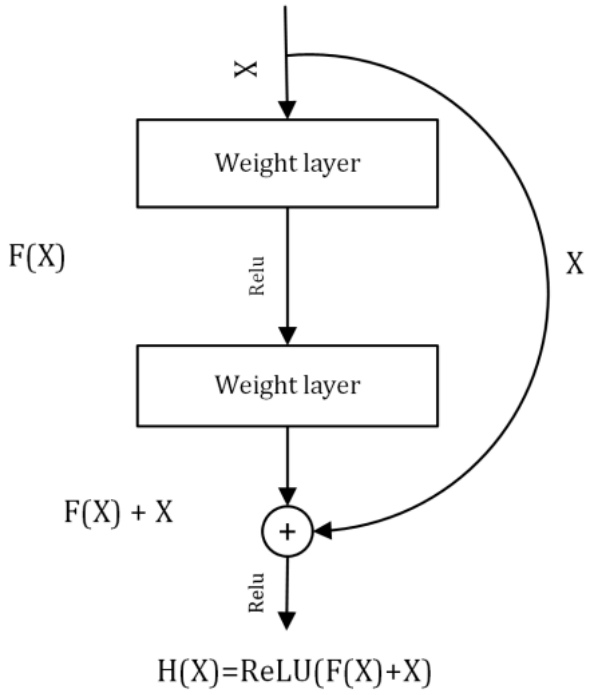

Figure 3: Deep residual network residual block

Initial convolution layers have filters of size 7 × 7 and 3 × 3, followed by max-pooling. The first group has three further parts or residual blocks each sub-block consists of 3 convolutional layers with a size of kernels 1 × 1, 3 × 3, and 1 × 1, respectively. The number of kernels used at each layer of the sub-block is 64, 64, and 128. The second group of layers has four residual blocks each consisting of 3 convolutional layers with a size of kernels 1 × 1, 3 × 3, and 1 × 1, respectively. The number of kernels used at each layer of the sub-block is 128, 128, and 512. The third group consists of 18 layers and six further residual blocks each consisting of 3 convolutional layers of the same size as in residual blocks 1 and 2. The number of kernels used at each layer of the sub-block is 256, 256, and 1024. Layers are stacked over one other with a different number of kernels. The fourth and final group consists of 9 layers and three residual blocks with each sub-block consisting of 3 convolutional layers with a size of kernels 1 × 1, 3 × 3, and 1 × 1, respectively. The number of kernels used at each layer of the sub-block is 512, 512, and 2048. The model uses average pooling and layers with the softmax for classification.

3. Different Measures used to evaluate Performance

The following quality measures were used to assess the suggested technique's performance:

3.1 Accuracy: This is the most basic metric and measures the proportion of correctly classified instances out of the total instances. It's calculated as:

Accuracy = (Number of Correct Predictions) / (Total Number of Predictions)

Formula:

Accuracy = (TP + TN) / (TP + TN + FP + FN)

Although accuracy offers a broad perspective on the overall model performance, it may not be the most suitable metric in scenarios involving imbalanced classes or situations where specific types of errors carry more significance than others.

3.2 Precision: Precision measures how many of the instances predicted as positive are actually positive. In other words, it focuses on the correctness of positive predictions. It's calculated as:

Precision = (True Positives) / (True Positives + False Positives)

Precision = TP / (TP + FP)

Elevated precision signifies that the model's positive class predictions are more likely to be correct. This aspect gains particular importance in circumstances where the impact of false positives holds substantial consequences.

3.3 Recall (Sensitivity or True Positive Rate): Recall evaluates the proportion of actual positive instances that were accurately predicted as positive. It gauges the model's capability to recognize all pertinent occurrences. The calculation for recall is as follows:

Recall = (True Positives) / (True Positives + False Negatives)

Recall = TP / (TP + FN)

A recall indicates that the model is proficient in identifying a substantial portion of the positive instances. This aspect becomes especially significant in scenarios where the implications of false negatives are significant.

3.4 F1 Score: The F1 score serves as an equilibrium metric that merges recall and precision into a unified measure. Calculated as the harmonic mean of recall and precision, it offers a well-rounded assessment by striking a balance between these two factors. The formula for calculating the F1 score is as follows:

F1 Score = 2 * (Precision * Recall) / (Precision + Recall)

The F1 score becomes valuable when you aim to account for both false positives and false

Negatives, seeking a singular metric that encapsulates a balance between these two aspects.

Results of one category of Skin cancer using skin lesion images are given in figure 4.

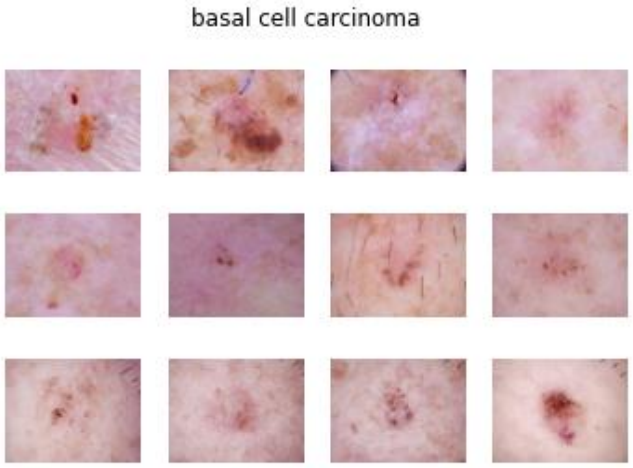

Figure 4: Shows basal cell carcinoma a type of skin cancer.

4 Confusion Matrix:

A confusion matrix provides a comprehensive overview of the accuracy of a machine-learning model. Its dimensions are determined by the number of classes to be predicted. The rows represent the algorithm's predictions, while the columns indicate the actual known values. In Figure 5, the top left corner represents the true positives, and the bottom right corner represents the true negatives. The bottom left corner corresponds to the false negatives, and the top right corner corresponds to the false positives.

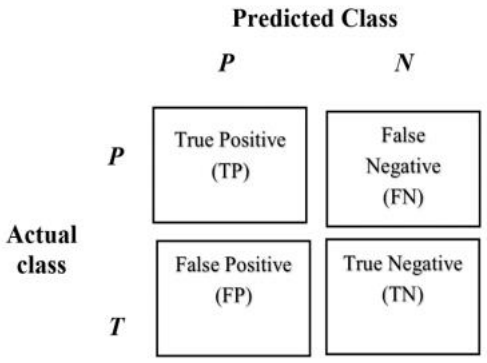

Figure 5: Confusion matrix of CNN model.

5. Conclusion

In this investigation, a deep learning classifier is employed to analyze cases of skin cancer disease. The input data for this analysis comprises instances of skin cancer disease, which undergo a pre-processing procedure. During pre-processing, the image data is resized and transformed into arrays. Subsequently, the data undergoes feature selection, which includes splitting the dataset into training and testing

subsets. Following this, all images are resized and converted into arrays. Ultimately, a classification technique is utilized to make predictions about the presence of skin cancer. The accuracy of this classification is determined using a deep learning convolutional neural network algorithm applied to image data, and maximum accuracy is given by the Resnet-50 model in less time which is 94.3%. The performance graph of the CNN model and Resnet-50 model shows in Graph 4.1 and Graph 4.2:

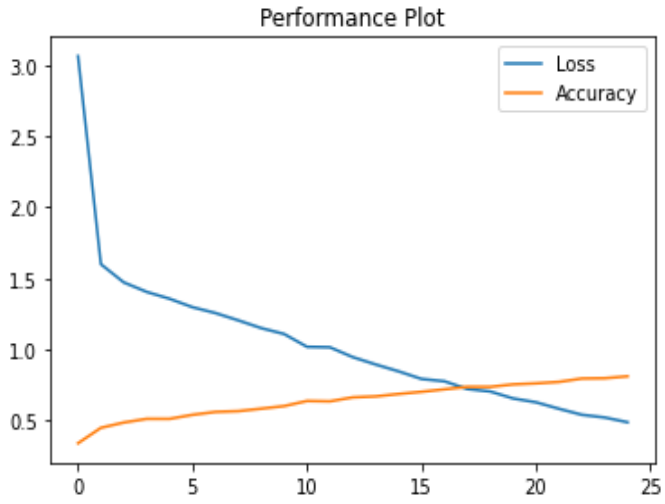

Graph 4.1: Performance plot of CNN Model

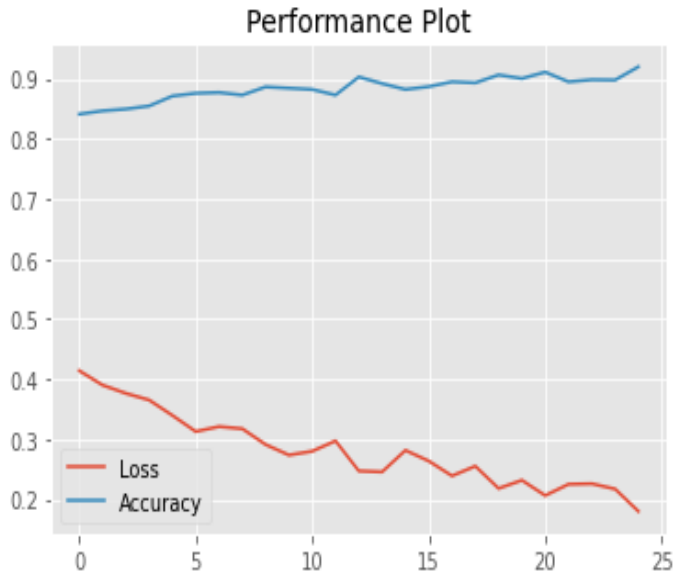

Graph 4.2: Representation of performance plot graph for Resnet-50 model.

Comparison Result of CNN model and Resnet-50 model shown in given Graph 5.1:

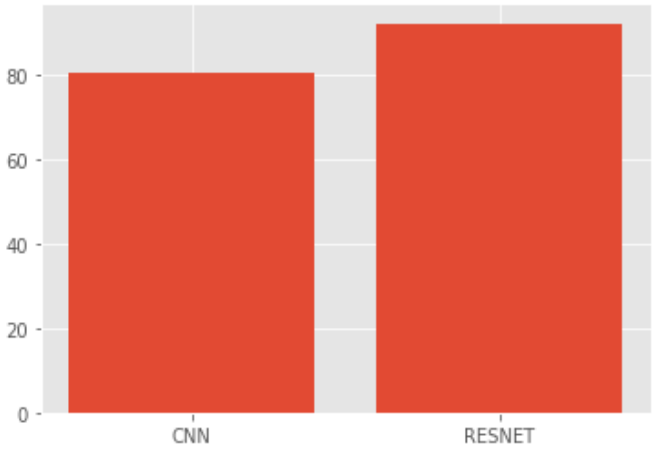

Graph 5.1: Shows the overall accuracy of CNN and Resnet-50 model.

REFERENCES

[1] P. Dubai, S. Bhatt, C. Joglekar, and S. Patii, "Skin cancer detection and classification," *Proc. 2017 6th Int. Conf. Electr. Eng. Informatics Sustain. Soc. Through Digit. Innov. ICEEI 2017*, vol. 2017-Novem, pp. 1–6, 2018, doi: 10.1109/ICEEI.2017.8312419.

[2] A. Imran, A. Nasir, M. Bilal, G. Sun, A. Alzahrani, and A. Almuhaimeed, "Skin Cancer Detection Using Combined Decision of Deep Learners," *IEEE Access*, vol. 10, pp. 118198–118212, 2022, doi: 10.1109/ACCESS.2022.3220329.

[3] P. R. Hill, H. Bhaskar, M. E. Al-Mualla, and D. R. Bull, "Improved illumination invariant homomorphic filtering using the dual tree complex wavelet transform," in *2016 IEEE International Conference on Acoustics, Speech and Signal Processing (ICASSP)*, 2016, pp. 1214–1218. doi: 10.1109/ICASSP.2016.7471869.

[4] A. Victor and D. M. Ghalib, "Automatic Detection and Classification of Skin Cancer," *Int. J. Intell. Eng. Syst.*, vol. 10, pp. 444–451, 2017, doi: 10.22266/ijies2017.0630.50.

[5] R. Moussa, F. Gerges, C. Salem, R. Akiki, O. Falou, and D. Azar, "Computer-aided detection of Melanoma using geometric features," in *2016 3rd Middle East Conference on Biomedical Engineering (MECBME)*, 2016, pp. 125–128. doi: 10.1109/MECBME.2016.7745423.

[6] N. F. M. Azmi, H. M. Sarkan, Y. Yahya, and S. Chuprat, "ABCD rules segmentation on malignant tumor and benign skin lesion images," in *2016 3rd International Conference on Computer and Information Sciences*

(ICCOINS), 2016, pp. 66–70. doi: 10.1109/ICCOINS.2016.7783190.

[7] G. Arora, A. K. Dubey, Z. A. Jaffery, and A. Rocha, "Architecture of an effective convolutional deep neural network for segmentation of skin lesion in dermoscopic images," *Expert Syst.*, no. January, pp. 1–13, 2021, doi: 10.1111/exsy.12689.

[8] S. Das and D. Das, "Skin Lesion Segmentation and Classification: A Deep Learning and Markovian Approach," in *2021 IEEE Mysore Sub Section International Conference (MysuruCon)*, 2021, pp. 546–551. doi: 10.1109/MysuruCon52639.2021.9641583.

[9] R. Mahum and S. Aladhadh, "Skin Lesion Detection Using Hand-Crafted and DL-Based Features Fusion and LSTM.," *Diagnostics (Basel, Switzerland)*, vol. 12, no. 12, Nov. 2022, doi: 10.3390/diagnostics12122974.

[10] G. . Jayalakshmi and S. Kumar, "Performance analysis of Convolutional Neural Network (CNN) based Cancerous Skin Lesion Detection System," 2019, pp. 1–6. doi: 10.1109/ICCIDS.2019.8862143.

[11] Y. Filali, S. Abdelouahed, and A. Aarab, "An improved segmentation approach for skin lesion classification," vol. 7, 2019, doi: 10.19139/soic.v7i2.533.

[12] A. Masood and A. A. Al-Jumaily, "Computer aided diagnostic support system for skin cancer: a review of techniques and algorithms.," *Int. J. Biomed. Imaging*, vol. 2013, p. 323268, 2013, doi: 10.1155/2013/323268.

[13] T. J. Brinker *et al.*, "Skin Cancer Classification Using Convolutional Neural Networks: Systematic Review.," *J. Med. Internet Res.*, vol. 20, no. 10, p. e11936, Oct. 2018, doi: 10.2196/11936.

[14] A. Saleem, N. Bhatti, A. Ashraf, M. Zia, and H. Mehmood, "Segmentation and classification of consumer-grade and dermoscopic skin cancer images using hybrid textural analysis.," *J. Med. imaging (Bellingham, Wash.)*, vol. 6, no. 3, p. 34501, Jul. 2019, doi: 10.1117/1.JMI.6.3.034501.

[15] V. S., J. C., P. Subhashini, and S. .K, "Image Enhancement and Implementation of CLAHE Algorithm and Bilinear Interpolation," *Cybern. Syst.*, pp. 1–13, 2022, doi: 10.1080/01969722.2022.2147128.

[16] M. A. Khan, M. I. Sharif, M. Raza, A. Anjum, T. Saba, and S. A. Shad, "Skin lesion segmentation and classification: A unified framework of deep neural network features fusion and selection," *Expert Syst.*, vol. 39, no. 7, pp. 1–21, 2022, doi: 10.1111/exsy.12497.

[17] U. B. Ansari and M. E. Student, "Skin Cancer Detection Using Image Processing Tanuja Sarode 2," *Int. Res. J. Eng. Technol.*, vol. 4, no. 4, pp. 2395–56, 2017, [Online]. Available: https://www.irjet.net/archives/V4/i4/IRJET-V4I4702.pdf

[18] F. Afza, M. Khan, M. Sharif, and A. Rehman, "Microscopic skin laceration segmentation and classification: A framework of statistical normal distribution and optimal feature selection," *Microsc. Res. Tech.*, vol. 82, 2019, doi: 10.1002/jemt.23301.

[19] A. Mahbod, G. Schaefer, I. Ellinger, R. Ecker, A. Pitiot, and C. Wang, "Fusing fine-tuned deep features for skin lesion classification," *Comput. Med. Imaging Graph.*, vol. 71, pp. 19–29, 2019, doi: https://doi.org/10.1016/j.compmedimag.2018.10.007.

[20] S.-T. Tran, C.-H. Cheng, T.-T. Nguyen, M.-H. Le, and D.-G. Liu, "TMD-Unet: Triple-Unet with Multi-Scale Input Features and Dense Skip Connection for Medical Image Segmentation.," *Healthc. (Basel, Switzerland)*, vol. 9, no. 1, Jan. 2021, doi: 10.3390/healthcare9010054.

[21] X. Wang, W. Huang, Z. Lu, and S. Huang, "Multi-level Attentive Skin Lesion Learning for Melanoma Classification," in *2021 43rd Annual International Conference of the IEEE Engineering in Medicine & Biology Society (EMBC)*, 2021, pp. 3924–3927. doi: 10.1109/EMBC46164.2021.9629858.

[22] S. Fernandes, V. Rajinikanth, and S. Kadry, "A Hybrid Framework to Evaluate Breast Abnormality Using Infrared Thermal Images," *IEEE Consum. Electron. Mag.*, vol. 8, pp. 31–36, 2019, doi: 10.1109/MCE.2019.2923926.

[23] M. A. Al-masni, M. A. Al-antari, H. M. Park, N. H. Park, and T.-S. Kim, "A Deep Learning Model Integrating FrCN and Residual Convolutional Networks for Skin Lesion Segmentation and Classification," in *2019 IEEE Eurasia Conference on Biomedical Engineering, Healthcare and Sustainability (ECBIOS)*, 2019, pp. 95–98. doi: 10.1109/ECBIOS.2019.8807441.

[24] H. Ragb and V. Asari, "Histogram of oriented phase (HOP): a new descriptor based on phase congruency," 2016, p. 98690V. doi: 10.1117/12.2225159.

[25] J. Bian, S. Zhang, S. Wang, J. Zhang, and J. Guo, "Skin Lesion Classification by Multi-View Filtered Transfer Learning," *IEEE Access*, vol. 9, pp. 66052–66061, 2021, doi: 10.1109/ACCESS.2021.3076533.

[26] R. Rout, P. Parida, and S. Patnaik, "Melanocytic Skin Lesion Extraction Using Mean Shift Clustering," in *2021 International Conference on Electronic Information Technology and Smart Agriculture (ICEITSA)*, 2021, pp. 565–574. doi: 10.1109/ICEITSA54226.2021.00112.

ABOUT AUTHOR

1'st Author Photo

KIRAN
M.TECH (Computer Science & Engineering)
Guru Nanak Dev Engineering College
Ludhiana , Punjab, INDIA

2nd Author Photo

GURJIT KAUR
Assistant Professor Department of Computer Science & Engineering
Guru Nanak Dev Engineering College
Ludhiana , Punjab, INDIA

3rd Author Photo

PRIYANKA ARORA
Assistant Professor Department of Computer Science & Engineering
Guru Nanak Dev Engineering College
Ludhiana , Punjab, INDIA